View Article Online
View Journal

Catalysis Science & Technology

This article can be cited before page numbers have been issued, to do this please use: Y. Ge, G. Cheng, N. Xu, W. Wang and H. Ke, *Catal. Sci. Technol.*, 2019, DOI: 10.1039/C9CY00739C.

ROYAL SOCIETY OF CHEMISTRY

rsc.li/catalysis

View Article Online
DOI: 10.1039/C9CY00739C

ARTICLE

Zinc 2-N-Methyl N-confused porphyrin: An Efficient Catalyst for the Conversion of CO_2 into Cyclic Carbonates

Received 00th January 20xx,
Accepted 00th January 20xx

DOI: 10.1039/x0xx00000x

Yuansheng Ge,[a] Guoe Cheng*,[a] Nanfeng Xu,[a] Weizhou Wang*,[b] and Hanzhong Ke*[a]

A zinc 2-N-Methyl N-confused porphyrin (Zn(NCP)Cl) catalyst was developed for the solvent-free synthesis of cyclic carbonates from epoxides and CO_2. Zn(NCP)Cl exhibited very high catalytic activity. Using this catalyst, a series of epoxides have been converted into the corresponding cyclic carbonates in high yields and selectivity (>99%). The turnover frequency (TOF) value reached 266667 h^{-1} for the conversion of CO_2 with epichlorohydrin into cyclic carbonate at 120 °C and an initial CO_2 pressure of 1.7 MPa within 3 h. Furthermore, almost quantitative cyclic carbonate product was achieved under atmospheric CO_2 within 24 h. X-ray structural analysis of Zn(NCP)Cl reveals that the Zn^{2+} ion is four-coordinate, surrounded by three nitrogen atoms from the N-confused porphyrin and a chlorine atom. Due to the strong electron-withdrawing ability of chloride, zinc shows strong acidity, thereby enhance its ability to activate epoxide. Density functional theory calculations (DFT) suggest that the ring-opening of epoxide is the rate-determine step of the catalytic cycle.

Introduction

Carbon dioxide (CO_2) is a waste product of many processes. The excessive emission of CO_2 into the atmosphere has result in serious global climate change. The conversion of CO_2 into valuable chemicals is a most worthwhile area due to the economic and environmental benefits in light of the problem of greenhouse effect and the renewable carbon resource.[1-4] One of the most important products of CO_2 transforming is cyclic carbonates (Scheme 1)[5] which have been widely used as organic synthetic intermediates,[6] polar aprotic solvents,[7] electrolytes in lithium ion batteries,[8] precursors for biomedical applications,[9-10] and as raw materials for engineering plastics.[11] As an attractive C_1 feedstock in organic synthesis, CO_2 is abundant, inexpensive, nontoxic, and nonflammable. Furthermore, the synthesis of cyclic carbonate from CO_2 and epoxide exhibits 100% atom efficiency.[12] However, the CO_2/epoxide coupling reaction is hindered due to the thermodynamic and kinetic stability of CO_2. In recent decades, much effort has been devoted to develop highly efficient and practical catalysts for this reaction, such as metal-based catalysts (for example, metal salen complexes,[13-19] metal porphyrins,[20-28] aluminum triphenolate complex,[29] alkali metal salts,[30] metal oxides,[31] Metal–Organic Frameworks[32]) and metal-free catalysts (for example, quaternary ammonium salts,[33-38] imidazolium salts,[39-45] phosphonium salts,[46-48] phenolic catalysts,[49-51] and ionic liquids[52-54]). Among these catalysts, the Lewis acidity of zinc compounds shows outstanding catalytic performance for the cycloaddition of CO_2 to epoxides. Maeda and co-workers reported that a zinc (II) porphyrin with quaternary ammonium bromides (nucleophiles) at the meta positions showed very high catalytic activity.[55] The TOF value of this catalyst reached 31500 h^{-1}, which is among the highest reported for monometallic complexes for the cycloaddition of CO_2 and epoxides to cyclic carbonates. According to the mechanism reported by the literatures,[56-58] activation of epoxides via coordination

---

[a] *Faculty of Materials Science and Chemistry, China University of Geosciences (Wuhan), Wuhan 430074, People's Republic of China.*
E-mail：chengge@cug.edu.cn; kehanz@163.com
[b] *College of Chemistry and Chemical Engineering, and Henan Key Laboratory of Function-Oriented Porous Materials, Luoyang Normal University, Luoyang 471934, People's Republic of China.*
E-mail：wzw@lynu.edu.cn

Electronic Supplementary Information (ESI) available: ^1H and ^{13}C NMR, FT-IR, HRMS spectra of Zn(NCP)Cl, typical procedure for the synthesis of cyclic carbonates, ^1H NMR spectra of cyclic carbonates, details of crystal data, DFT calculations.

View Article Online
DOI: 10.1039/C9CY00739C

with metal center is critical in these metal catalytic reactions. It is well understood that the reactivity of such metal catalysts is strongly dependent on their Lewis acidity.

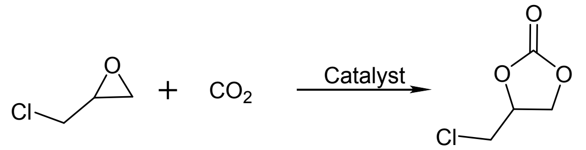

Scheme 1. The Cycloaddition of epichlorohydrin and CO_2

N-confused porphyrin is a porphyrin isomer with an inverted pyrrole ring. Different from the N4 coordinated sites of porphyrin, such an exotic porphyrin provide N3 or N3C coordinated sites to form two kinds of metal complexes.[59-61] Zinc 2-N-Methyl N-confused porphyrin (Zn(NCP)Cl) (see Scheme 2) has a zinc-chlorine bond as well as three zinc-nitrogen bonds (see figure 1). The strong electron-withdrawing ability of chloride can enhance the acidity of zinc.[62] We reasoned that Zn(NCP)Cl with a more Lewis acidic metal center is a new powerful catalyst. In this context, we reported the catalytic activity of Zn(NCP)Cl as the first example of metal N-confused porphyrin for the conversion of CO_2 into cyclic carbonates.

Result and discussion

Scheme 2 shows the chemical structure and the strategy for the synthesis of Zn(NCP)Cl discussed in the present study. The complex Zn(NCP)Cl can be easily synthesized in 49% yield by reacting NCP with excess $ZnCl_2$ in CH_3CN. The newly synthesized compound Zn(NCP)Cl was characterized by ^1H NMR and ^{13}C NMR. The ^1H NMR spectrum (in $CDCl_3$) of Zn(NCP)Cl showed a singlet at $\delta = -0.59$ ppm for the H(3) proton. This confirms that there is no coordinated bond between Zn and C(3) in Zn(NCP)Cl. The MALDI-TOF high resolution mass spectra (HRMS) of Zn(NCP)Cl exhibits $[M\text{-}Cl]^+$ peak at 691.1808, which deviate by 3.7617 ppm from the theoretical value of 691.1834. The solid-state structure of Zn(NCP)Cl was ascertained by X ray crystallography. The compound crystallized in the I 2/a space group. A perspective view of Zn(NCP)Cl is depicted in Figure 1. The geometry about Zn is distorted tetrahedral. The Zn atom in the core were tetracoordinated with three pyrrolic nitrogens, N(2), N(3), and N(4), and an axial Cl anionic ligand. The bond length between Zn and N(2), N(3) and N(4) atoms are 2.105(4), 2.011(4) and 2.107(4) Å, and the Cl-Zn bond length is 2.2575(15) Å. The strong electron-withdrawing ability of chloride can enhance the acidity of zinc. The Zn···C(3) distance is 2.506(5) Å, This value is much longer than the normal Zn-C bond distance found, hence, there is no direct interaction between Zn and C(3).[63] The Zn center is displaced by 0.592 Å out of the 3N mean plane formed by N((2)-N(3)-N(4) toward the axial chloride. The chloride ligand occupies the equatorial position with a N(3)-Zn-Cl angle of 119.33(13)°. The larger N(3)-Zn-Cl angle indicates that the axial ligand leans more toward the inverted pyrrole ring in Zn(NCP)Cl, which gives a more tetrahedral-like metal center rather than square-pyramidal, as found in tetracoordinated Zn porphyrin complexes. The confused pyrrole ring sharply tilted away from the plane defined by the tri-pyrrole unit and the dihedral angle between the confused pyrrole plane and the 3N plane is 49.55° (for details of crystal data, see the Supporting Information).

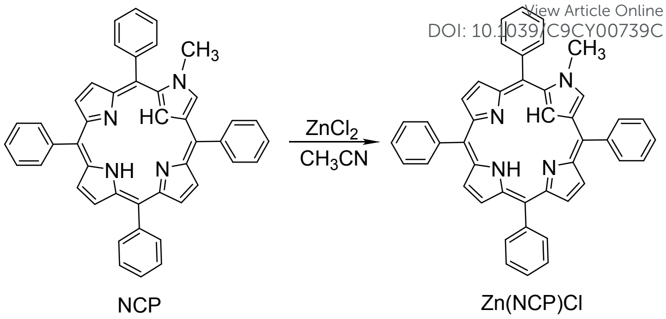

Scheme 2 Synthesis of Zn(NCP)Cl

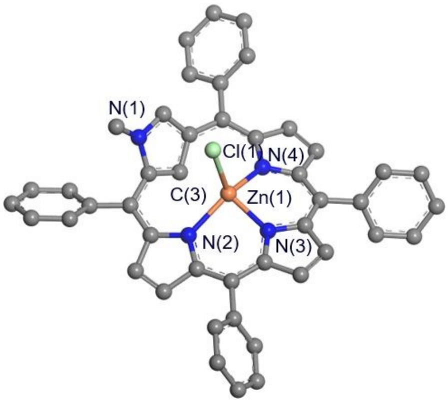

Figure 1. X-Ray structure of Zn(NCP)Cl. Hydrogen atoms are omitted for clarity. Selected bond lengths [Å] and bond angles [°]: Zn(1)-N(2), 2.105(4); Zn(1)-N(3), 2.011(4); Zn(1)-N(4), 2.107(4); Zn(1)-Cl(1), 2.2575(15); Zn(1)⋯C(3), 2.506(5); N(2)-Zn(1)-N(3), 89.24(15); N(3)-Zn(1)-N(4), 89.76(16); N(2)-Zn(1)-N(4), 146.07(16); N(2)-Zn(1)-Cl(1), 105.98(12); N(3)-Zn(1)-Cl(1), 119.33(13); N(4)-Zn(1)-Cl(1), 103.99(12).

The catalytic activities of this catalyst were initially investigated for the cycloaddition of CO_2 to epichlorohydrin under solvent-free conditions in combination with tetrabutylammonium bromide (TBAB) as a cocatalyst. The results are summarized in Table 1. It could be found that Zn(NCP)Cl was an efficient catalyst with high selectivity (>99%) for the coupling reaction of CO_2 and epichlorohydrin to chloropropene carbonate. When the catalyst and TBAB amounts were 0.0001 mol % and 0.016 mol %, respectively, 80% yield was obtained with a TOF of 266667 h^{-1} (Table 1, Entry 1). In order to avoid any substrate effects (such as high volatility), the cycloaddition of CO_2 and Phenyl glycidyl ether (Boiling point: 245-247 ^{o}C) was also investigated at the same conditions. The yield and TOF reached 81% and 270000 h^{-1} (Table 1, Entry 17), respectively. At a catalyst loading of 0.004 mol% and a TBAB loading of 0.016 mol %, almost quantitative cyclic carbonate product (98%) of this was achieved within 3 h (Table 1, Entry 3). When the reaction time was shortened to 1 h, the yield was still up to 89% (Table 1, Entry 5). Ema reported that metalloporphyrins have excellent catalytic activity for the cycloaddition of CO_2 to epoxide.[25] For comparison, a catalytic system composed of (5,10,15,20-tetraphenylporphyrinato)Zinc (Zn(TPP)) and TBAB was evaluated under the same conditions. Only 79% product of cyclic carbonate was obtained with a TOF of 6583 h^{-1} (Table 1, Entry 16).

Table 1. Catalytic data for Zn(NCP)Cl catalyzed reactions of CO_2 with epichlorohydrin^{a}

Entry	Zn(NCP)Cl (mol %)	cocat.	*t* (h)	*T* (^{o}C)	*P* (MPa)	yield.^{b,c} (%)	TOF (h^{-1})
1	0.0001	TBAB	3	120	1.7	80	266667
2	0.002	TBAB	3	120	1.7	92	15333
3	0.004	TBAB	3	120	1.7	98	8167
4	0.004	TBAB	2	120	1.7	92	11500
5	0.004	TBAB	1	120	1.7	89	22250
6	0.004	TBAB	3	100	1.7	90	7500
7	0.004	TBAB	3	80	1.7	51	4250
8	0.004	TBAB	3	65	1.7	24	2000
9	0.004	TBAB	3	120	1.0	96	8000
10	0.004	TBAB	3	120	0.5	92	7667
11^{d}	0.004	TBAB	24	120	0.1	97	1010
12	-	TBAB	3	120	1.7	19	
13	0.004	-	3	120	1.7	13	1083
14	0.004	TBAC	3	120	1.7	69	5750
15	0.004	TBAI	3	120	1.7	74	6167
16^{e}	0.004	TBAB	3	120	1.7	79	6583
17^{f}	0.0001	TBAB	3	120	1.7	81	270000

Reaction conditions: ^{a}Epichlorohydrin (3.13 mL, 40 mmol), cocatalyst (0.016 mol %), 100 mL autoclave. ^{b}Determined by ^{1}H NMR using mesitylene as an internal standard. ^{c}Selectivity for the cyclic carbonate product >99%. ^{d}The reaction was carried out in a 100 mL three-neck flask under CO_2 atmosphere. ^{e}Using Zn(TPP) instead of Zn(NCP)Cl as catalyst. ^{f}Using Phenyl glycidyl ether as a substrate.

The effect of reaction temperature on the cycloaddition of CO_2 and epichlorohydrin to chloropropene carbonate was investigated in the temperature range of 65-120°C (Table 1, entries 3, 6-8). under the identical conditions (catalyst loading, 0.004 mol%; TBAB loading, 0.016 mol%; CO_2 pressure, 1.7 MPa; 3 h), the yield of chloropropene carbonate increased with the elevation of temperature from 65 °C to 120 °C. The yields at 65°C, 80°C, 100°C and 120°C were 24%, 51%, 90% and 98%, respectively.

The effect of CO_2 pressure on the catalytic performance was also examined under the identical conditions (catalyst loading, 0.004 mol%; TBAB loading, 0.016 mol%; 120 °C; 3 h) (Table 1, entries 3, 9-10). The yields retained nearly constant (>92%) at initial CO_2 pressure in the range of 0.1-1.7 MPa, suggesting that

View Article Online
DOI: 10.1039/C9CY00739C

CO_2 was not the rate-determining step in this pressure range. To our excitement, almost quantitative yield (97%) of cyclic carbonate was obtained under atmospheric CO_2 within 24 h (Table 1, entry11).

The role of co-catalyst TBAB was found to be quite important.[64] When TBAB and Zn(NCP)Cl were used alone as catalysts for the coupling reaction of CO_2 and epichlorohydrin, the yields were only 19% (Table 1, entry 12) and 13% (Table 1, entry 13), respectively. However, when Zn(NCP)Cl/TBAB was used as catalyst, a quantitative cyclic carbonate product was achieved. These results indicated that the presence of both Zn(NCP)Cl and TBAB was necessary for high efficiency. The metal center and Br^- anion acted as a Lewis acid and a Lewis base or nucleophile, and Both worked cooperatively to open the epoxide ring. The effect of the X^- anion on the catalytic activity was examined by using TBAB, tetrabutylammonium chloride (TBAC), and tetrabutylammonium iodide (TBAI) as the cocatalyst (Table 1, entries 3, 14-15). The order of catalytic activity is TBAB (98%) > TBAI (74%) >TBAC (69%). TBAB showed much higher catalytic activity than TBAI and TBAC.

On the basis of our experimental results and the mechanism reported by the literatures,[65-67] we propose the catalytic cycle shown in Scheme 3. In the catalytic cycle, the epoxide is first activated via coordination with Lewis acidic Zn center. The Lewis acidic Zn center can activate the C–O bond of the epoxide to facilitate ring-opening. Then, nucleophilic attack by Br^- ion on the less hindered side of the epoxide produces the metal alkoxide intermediate via a ring-opening reaction, which is followed by CO_2 insertion and intramolecular ring closure to produce the cyclic carbonate and the catalyst is regenerated.

To gain deeper insight into the reaction mechanism, we performed DFT calculations along the proposed reaction pathway (Scheme 3). The assistance of the quaternary ammonium salt was simulated by including only the bromine anion, and epichlorohydrin was used as a substrate. The free energy profile calculated for the reaction catalyzed by Zn(NCP)Cl/TBAB is shown in Figure 2. The optimized structures for the reactant, intermediates, transition states and product in the catalyzed reaction are shown in Figure 3. At the first step of the catalytic cycle, lewis acidic Zn center activated the epichlorohydrin and the nucleophilic Br^- attacking to the least substituted carbon atom of epichlorohydrin leads to the formation of the metal alkoxide intermediate Int1 with an energy barrier of 15.6 kcal mol^{-1}. And the release of the chloride anion via transition state TS2, with an energy barrier of 4.9 kcal mol^{-1}. The relative free energy of Int2 is 3.4 kcal mol^{-1} below the reference energy of Int1. This energy stabilization is caused by strong interaction between the negatively charged oxygen atom and the positive Zinc center. The addition of the CO_2 molecule leads to the formation of the intermediate int3. Subsequently, CO_2 insertion and intramolecular ring closure leads to the formation of the product-coordinated intermediate Int4. This step proceeds via transition state TS4 by surmounting an energy barrier of 15.1 kcal mol^{-1}. The relative free energy of transition state TS4 is 22.2 kcal/mol, which is reasonably in line with the kinetic data presented in Table 1, entry 8 (slow reaction at 65 °C). Finally, the dissociation of cyclic carbonate from Int4 and regeneration of the Zn(NCP)Cl complex allows further ECH turnover. The overall reaction was calculated to be exergonic by 9.7 kcal mol^{-1}.

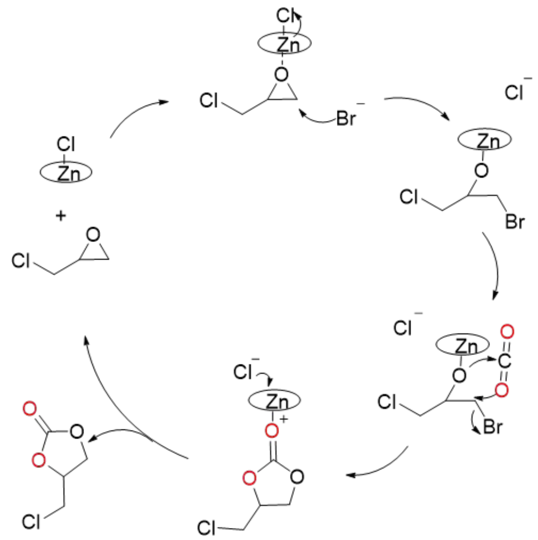

Scheme 3. A Proposed mechanism for the coupling of epoxide and CO_2 catalyzed by Zn(NCP)Cl/TBAB

View Article Online
DOI: 10.1039/C9CY00739C

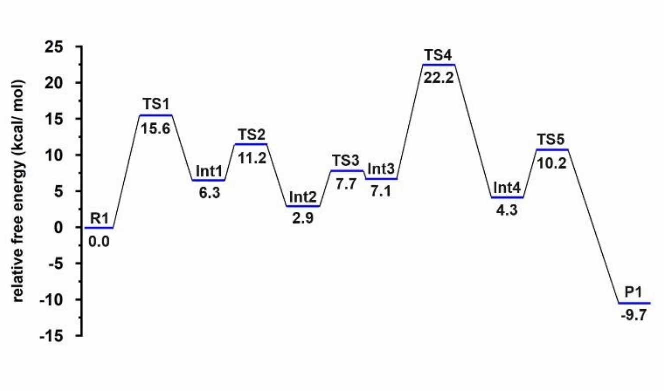

Figure 2. B3LYP-D3 free energy profile for the cycloaddition of CO_2 with epichlorohydrin catalyst by Zn(NCP)Cl/TBAB. The relative energies are given in kcal mol^{-1} and relative to the R1. TBAB is simulated by including only the bromine anion.

To investigate the general applicability of Zn(NCP)Cl, terminal epoxides (propylene oxide, epichlorohydrin, ethylethylene oxide, isobutylene oxide, styrene oxide) and internal epoxides (1,2-dimethylethylene oxide, cyclohexene epoxide) were used as substrates at the identical conditions (catalyst loading, 0.02 mol%; TBAB loading, 0.08 mol%; CO_2 pressure, 1.7 MPa; 120 °C) and the results are summarized in Table 2. At a low catalyst loading (0.02 mol %), these epoxides could be converted into the corresponding cyclic carbonates with high selectivities (>99%) and excellent yields, indicating the high versatility of this catalyst system. Our catalyst system showed high-activity towards terminal epoxides. Propylene oxide (Table 2, entry 1), epichlorohydrin (Table 2, entry 2) and isobutylene oxide (Table 2, entry 4) were quantitatively converted into corresponding cyclic carbonates within 3 h, while ethylene oxide (Table 2, entry 3) and styrene oxide (Table 2, entry 5) within 6 h. To achieve 99 % yield, ethylethylene oxide took longer time than propylene oxide, which could be attributed to the electron-donating effect of the ethyl group and its steric hindrance that obstructed the approach of ethylethylene oxide towards the catalytic site. For internal cyclohexene oxide, 92% yield was achieved after a reaction time of 12 h (Table 2, entry 6). For 1,2-dimethylethylene oxide, it also showed the presentable catalytic performance (Table 2, entry 7).

Conclusions

In summary, Zn(NCP)Cl/TBAB was proved to be an excellent catalyst system for the coupling of CO_2 with epoxides to conversion cyclic carbonates selectively under solvent-free conditions. The TOF value of this

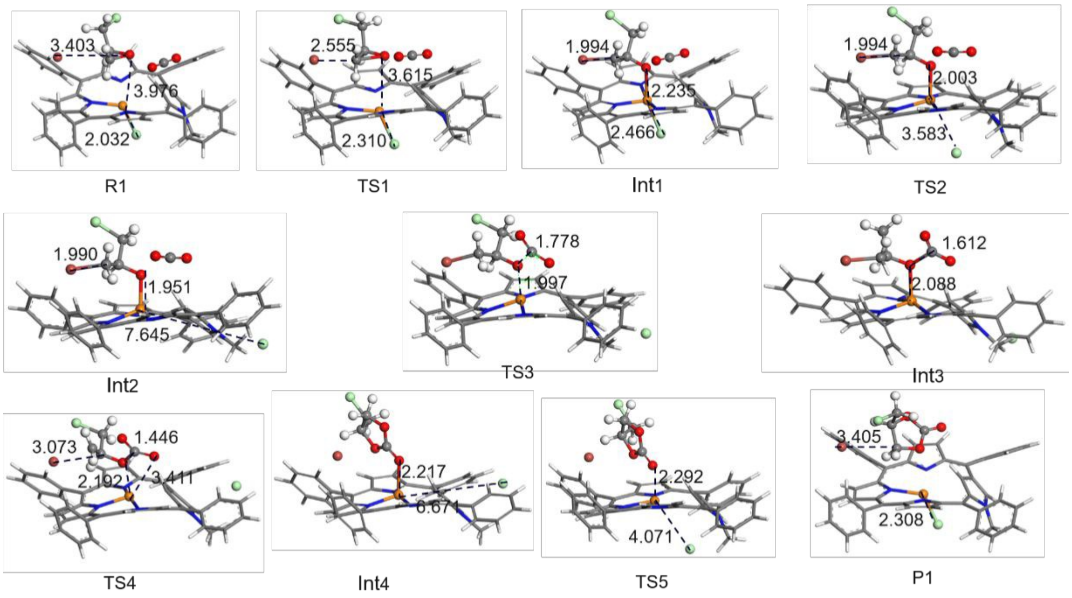

Figure 3. Optimized structures for the reactant, intermediates, transition states and product. Interatomic distances are in Å. Grey=carbon, white=hydrogen, blue=nitrogen, red=oxygen, yellow=zinc, green=chloride, brown=bromine.

Table 2. Cycloaddition of CO_2 with Various Epoxides

Entry	Epoxide	Product	t(h)	Yield (%)
1		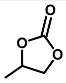	3	99

View Article Online
DOI: 10.1039/C9CY00739C

2	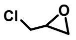	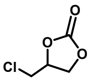	3	99
3	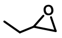	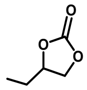	6	99
4	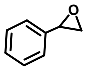	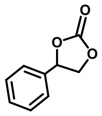	3	99
5		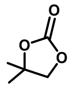	6	99
6	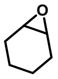	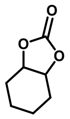	12	92
7		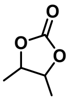	12	68

Reaction conditions: Epoxide (40.0 mmol), catalyst (0.02 mol %, 5.83 mg, 0.008 mmol), TBAB (0.08 mol %, 10.32 mg, 0.032 mmol), CO_2 (1.7 MPa), 120 °C. The yield was determined by ^1H NMR using mesitylene as an internal standard. The selectivity for the cyclic carbonate product >99%.

catalyst reached 266667 h^{-1} for the conversion of CO_2 with epichlorohydrin into cyclic carbonate at 120 °C and an initial CO_2 pressure of 1.7 MPa within 3 h. We demonstrated that almost quantitative cyclic carbonate product was achieved under atmospheric CO_2 within 24 h. Furthermore, this catalyst also displays a wide substrate scope. X-ray structural analysis of Zn(NCP)Cl reveals that the Zn^{2+} ion is four-coordinate with three nitrogen atoms and one chlorine atom. Due to the strong electron-withdrawing ability of chloride, zinc shows strong acidity, thereby enhance its ability to activate epoxide. A possible mechanism was proposed and supported by the results of DFT calculations. DFT calculations reveal that the ring-opening of epoxide by zinc is the rate-determine step of the catalytic cycle.

Experimental

General

All epoxide substrates and reagents were purchased from Energy Chemical (China) and used as received unless stated otherwise. Carbon dioxide (99.999%) was purchased from Wuhan Iron and Steel Group Gas Company and used without further purification. Solvents were dried according to standard procedures, distilled, and deaerated prior to use. NCP was synthesized by following the literature procedure.[68] NMR spectra were recorded with a Bruker Avance III HD 400 MHz spectrometer. ^1H NMR chemical shifts are reported relative to TMS (δ=0.00 ppm) and ^{13}C NMR chemical shifts are reported relative to $CDCl_3$ (δ=77.16 ppm). High-resolution mass spectra, reported as m/z, were obtained with a Bruker Autoflex MALDI-TOF mass spectrometer. FT-IR spectra were recorded with a Bruker Vertex 70 FT-IR spectrometer.

Synthesis of Zn(NCP)Cl

A mixture of NCP (315 mg, 0.5 mmol) and $ZnCl_2$ (680 mg, 5 mmol) were refluxed in CH_3CN (50 mL) for 12 h. After removing the solvent, the residue was purified by column chromatography on silica gel using $CHCl_3$/MeOH (v/v, 50:1) as the eluent. The yield was 180 mg (49 %). MALDI-TOF HRMS: calcd. for $[M-Cl]^+$ 691.1834, found 691.1808. ^1H NMR (400 MHz, $CDCl_3$): δ = – 0.59 (s, 1H), 3.23 (s, 3H), 6.24 (s, 1H), 7.59 (s, 6H), 7.68–7.85 (m, 14H), 8.11–8.14 (m, 4H), 8.27-8.28 (d, J = 4 Hz, 2H), 8.33-8.34 (d, J = 4 Hz, 2H). ^{13}C NMR (400 MHz, $CDCl_3$): δ = 163.46, 162.91, 154.55, 153.69, 143.53, 143.09, 141.72, 141.30, 140.72, 136.29, 134.99, 134.85, 134.70, 133.58, 133.45, 131.70, 130.88, 130.48, 129.30, 129.06, 128.33, 127.90, 127.76, 127.20, 126.71, 124.05, 115.81, 115.27, 106.21, 38.83. FT-IR (KBr, cm^{-1}): 2922, 2852, 1596, 1546, 1502, 1259, 1070, 997, 796, 709.

General procedure for the synthesis of cyclic carbonates

The respective epoxide (40.0 mmol), Zn(NCP)Cl and TBAB were charged into a 100 mL stainless steel autoclave equipped with a magnetic stir bar. The autoclave was subjected to three cycles of pressurization and depressurization with carbon dioxide, and then pressurized to the required carbon dioxide pressure. The reaction mixture was heated with stirring to the required temperature. At the end of the reaction, the reactor was cooled down to room temperature with an ice bath before the excess CO_2 was released. The yield was determined by means of ^1H NMR using mesitylene as an internal standard. The products were purified using column chromatography with ethyl acetate/n-hexane (v/v, 1:4) as the eluent (for typical procedure, see the Supporting Information).

X-ray Crystallography

Single crystals of Zn(NCP)Cl suitable for X-ray diffraction study were grown by slow diffusion of hexanes into a CH$_2$Cl$_2$ solution of Zn(NCP)Cl at room temperature. The XRD crystal X-ray data were collected at 273 K using a Bruker SMART APEX diffractometer with MoKα radiation (λ= 0.71073 Å) and a graphite monochromator operating in multi-scan mode. Using Olex2,[69] the structure was solved with the SIR2004[70] structure solution program using Direct Methods and refined with the ShelXL[71] refinement package using Least Squares minimization. All non-hydrogen atoms were refined with anisotropic displacement parameters. Hydrogen atoms were placed in their idealized positions and allowed to ride on the respective carbon atoms. The single-crystal data are listed in Table S1.

CCDC-1902277 contains the supplementary crystallographic data for compound Zn(NCP)Cl. These data can be obtained free of charge from The Cambridge Crystallographic Data Centre via www.ccdc.cam.ac.uk/data_request/cif.

Computational methods

All the DFT calculations were carried out with the Gaussian 09 quantum chemistry package in the electronic ground states of the systems studied.[72] The molecular geometries were optimized at the B3LYP-D3/6-31G(d) theory level.[73] The reliability of the B3LYP-D3/6-31G(d) method can be found elsewhere.[74] Frequency calculations at the same level of theory were also performed to identify all stationary points as minima (zero imaginary frequencies) or transition states (one imaginary frequency). The transition states involved were checked by intrinsic reaction coordinate analysis.

Conflicts of interest

There are no conflicts of interest to declare.

Acknowledgements

This work was supported financially by the National Science Foundation of China (Grant no. 21777149). Computer time was provided by National Supercomputing Center in Shenzhen.

Notes and references

1 M. Cokoja, C. Bruckmeier, B. Rieger, W. A. Herrmann and F. E. Kuhn, *Angew. Chem. Int. Ed*, 2011, **50**, 8510-8537.

2 M. North and P. Styring, *Faraday Discuss*, 2015, **183**, 489-502.

3 Q. Liu, L. Wu, R. Jackstell and M. Beller, *Nat. Commun*, 2015, **6**, 5933-5948.

4 M. Alves, B. Grignard, R. Mereau, C. Jerome, T. Tassaing and C. Detrembleur, *Catal. Sci. Technol*, 2017, **7**, 2651-2684.

5 A. Decortes, A. M. Castilla and A. W. Kleij, *Angew. Chem. Int. Ed*, 2010, **49**, 9822-9837.

6 H. Matsukizono and T. Endo, *J. Am. Chem. Soc*, 2018, **140**, 884-887.

7 B. Schäffner, F. Schäffner, S. P. Verevkin and A. Börner, *Chem. Rev.*, 2010, **110**, 4554-4581.

8 K. Xu, Chem. Rev., 2004, **104**, 4303−4417.

9 V. Laserna, G. Fiorani, C. J. Whiteoak, E. Martin, E. Escudero-Adan and A. W. Kleij, *Angew. Chem. Int. Ed*, 2014, **53**, 10416-10419.

10 Z. Han, L. Rong, J. Wu, L. Zhang, Z. Wang and K. Ding, *Angew. Chem. Int. Ed*, 2012, **51**, 13041-13045.

11 L. Maisonneuve, A.-L. Wirotius, C. Alfos, E. Grau and H. Cramail, *Polym. Chem.*, 2014, **5**, 6142-6147.

12 J. A. Kozak, J. Wu, X. Su, F. Simeon, T. A. Hatton and T. F. Jamison, *J. Am. Chem. Soc*, 2013, **135**, 18497-18501.

13 M. North and C. Young, *Catal. Sci. Technol*, 2011, **1**, 93-99.

14 J. A. Castro-Osma, A. Lara-Sánchez, M. North, A. Otero and P. Villuendas, *Catal. Sci. Technol*, 2012, **2**, 1021-1026.

15 P. P. Pescarmona and M. Taherimehr, *Catal. Sci. Technol*, 2012, **2**, 2169-2187.

16 D. Tian, B. Liu, Q. Gan, H. Li and D. J. Darensbourg, *ACS Catal*, 2012, **2**, 2029-2035.

17 J. Chun, S. Kang, N. Kang, S. M. Lee, H. J. Kim and S. U. Son, *J. Mater. Chem. A*, 2013, **1**, 5517.

18 J. A. Castro-Osma, C. Alonso-Moreno, A. Lara-Sánchez, J. Martínez, M. North and A. Otero, *Catal. Sci. Technol.*, 2014, **4**, 1674-1684.

19 J. Li, Y. Ren, C. Yue, Y. Fan, C. Qi and H. Jiang, *ACS Appl. Mater. Interfaces*, 2018, **10**, 36047-36057.

20 R. L. Paddock, Y. Hiyama, J. M. McKay and S. T. Nguyen, *Tetrahedron Lett*, 2004, **45**, 2023-2026.

21 L. Jin, H. Jing, T. Chang, X. Bu, L. Wang and Z. Liu, *J. Mol. Catal. A: Chem*, 2007, **261**, 262-266.

22 C. E. Anderson, S. I. Vagin, W. Xia, H. Jin and B. Rieger, *Macromolecules*, 2012, **45**, 6840-6849.

23 T. Ema, Y. Miyazaki, S. Koyama, Y. Yano and T. Sakai, *Chem. Commun*, 2012, **48**, 4489-4491.

View Article Online
DOI: 10.1039/C9CY00770C

24 K. Nakano, K. Kobayashi, T. Ohkawara, H. Imoto and K. Nozaki, *J. Am. Chem. Soc*, 2013, **135**, 8456-8459.

25 T. Ema, Y. Miyazaki, J. Shimonishi, C. Maeda and J. Y. Hasegawa, *J. Am. Chem. Soc*, 2014, **136**, 15270-15279.

26 C. Maeda, Y. Miyazaki and T. Ema, *Catal. Sci. Technol*, 2014, **4**, 1482-1497.

27 P. Li and Z. Cao, *Organometallics*, 2018, 37, 406-414.

28 J. V. Olsson, D. Hult, Y. Cai, S. García-Gallego and M. Malkoch, *Polym. Chem.*, 2014, **5**, 6651-6655.

29 C. J. Whiteoak, N. Kielland, V. Laserna, E. C. Escudero-Adan, E. Martin and A. W. Kleij, *J. Am. Chem. Soc*, 2013, **135**, 1228-1231.

30 L. Guo, C. Wang, X. Luo, G. Cui and H. Li, *Chem. Commun*, 2010, **46**, 5960-5962.

31 T. Yano, H. Matsui, T. Koike, H. Ishiguro, H. Fujihara, M. Yoshihara and T. Maeshima, *Chem. Commun.*, 1997, **12**, 1129–1130.

32 H. H. Wang, L. Hou, Y. Z. Li, C. Y. Jiang, Y. Y. Wang and Z. Zhu, *ACS Appl. Mater. Interfaces.*, 2017, **9**, 17969-17976.

33 M. Hong, Y. Kim, H. Kim, H. J. Cho, M. H. Baik and Y. Kim, *J. Org. Chem*, 2018, **83**, 9370-9380.

34 F. de la Cruz-Martínez, J. Martínez, M. A. Gaona, J. Fernández-Baeza, L. F. Sánchez-Barba, A. M. Rodríguez, J. A. Castro-Osma, A. Otero and A. Lara-Sánchez, *ACS Sustainable Chem. Eng*, 2018, **6**, 5322-5332.

35 F. D. Bobbink, D. Vasilyev, M. Hulla, S. Chamam, F. Menoud, G. Laurenczy, S. Katsyuba and P. J. Dyson, *ACS Catal*, 2018, **8**, 2589-2594.

36 M. Alves, B. Grignard, S. Gennen, C. Detrembleur, C. Jerome and T. Tassaing, *RSC Adv.*, 2015, **5**, 53629-53636.

37 T. Ema, K. Fukuhara, T. Sakai, M. Ohbo, F.-Q. Bai and J.-y. Hasegawa, *Catal. Sci. Technol*, 2015, **5**, 2314-2321.

38 A. Mirabaud, J.-C. Mulatier, A. Martinez, J.-P. Dutasta and V. Dufaud, *ACS Catal*, 2015, **5**, 6748-6752.

39 Y. Xie, J. Liang, Y. Fu, M. Huang, X. Xu, H. Wang, S. Tu and J. Li, *J. Mater. Chem. A*, 2018, **6**, 6660-6666.

40 N. Liu, Y.-F. Xie, C. Wang, S.-J. Li, D. Wei, M. Li and B. Dai, *ACS Catal*, 2018, **8**, 9945-9957.

41 S. Jayakumar, H. Li, J. Chen and Q. Yang, *ACS Appl. Mater. Interfaces*, 2018, **10**, 2546-2555.

42 M. Ding and H. L. Jiang, *ACS Catal*, 2018, **8**, 3194-3201.

43 T. Wang, W. Wang, Y. Lyu, X. Chen, C. Li, Y. Zhang, X. Song and Y. Ding, *RSC Adv.*, 2017, **7**, 2836-2841.

44 D. Wei-Li, J. Bi, L. Sheng-Lian, L. Xu-Biao, T. Xin-Man and A. Chak-Tong, *Catal. Sci. Technol.*, 2014, **4**, 556-562.

45 L. A. Bivona, O. Fichera, L. Fusaro, F. Giacalone, M. Buaki-Sogo, M. Gruttadauria and C. Aprile, *Catal. Sci. Technol*, 2015, **5**, 5000-5007.

46 B. Chatelet, L. Joucla, J. P. Dutasta, A. Martinez, K. C. Szeto and V. Dufaud, *J. Am. Chem. Soc*, 2013, **135**, 5348-5351.

47 B. Chatelet, L. Joucla, J.-P. Dutasta, A. Martinez and V. Dufaud, *J. Mater. Chem. A*, 2014, **2**, 14164-14172.

48 Y. Toda, Y. Komiyama, A. Kikuchi and H. Suga, *ACS Catal*, 2016, **6**, 6906-6910.

49 X. Wu, C. Chen, Z. Guo, M. North and A. C. Whitwood, *ACS Catal*, 2019, **9**, 1895-1906.

50 Y. Chen, R. Luo, J. Bao, Q. Xu, J. Jiang, X. Zhou and H. Ji, *J. Mater. Chem. A*, 2018, **6**, 9172-9182.

51 N. Zhang, B. Zou, G.-P. Yang, B. Yu and C.-W. Hu, *J. CO_2. Util*, 2017, **22**, 9-14.

52 Y. Zhi, P. Shao, X. Feng, H. Xia, Y. Zhang, Z. Shi, Y. Mu and X. Liu, *J. Mater. Chem. A*, 2018, **6**, 374-382.

53 J. Cao, W. Shan, Q. Wang, X. Ling, G. Li, Y. Lyu, Y. Zhou and J. Wang, *ACS Appl. Mater. Interfaces*, 2019, **11**, 6031-6041.

54 L.-G. Ding, B.-J. Yao, F. Li, S.-C. Shi, N. Huang, H.-B. Yin, Q. Guan and Y.-B. Dong, *J. Mater. Chem. A*, 2019, **7**, 4689-4698.

55 C. Maeda, J. Shimonishi, R. Miyazaki, J. Y. Hasegawa and T. Ema, *Chem. Eur. J*, 2016, **22**, 6556-6563.

56 J. Y. Hasegawa, R. Miyazaki, C. Maeda and T. Ema, *Chem. Rec*, 2016, **16**, 2260-2267.

57 R. I. Del, P. Brignou, S. M. Guillaume, J.-F. Carpentier and L. Maron, *Polym. Chem.*, 2011, **2**, 2564-2573.

58 X. Jiang, F. Gou, F. Chen and H. Jing, *Green Chem.*, 2016, **18**, 3567-3576.

59 J. Harvey, *Coord. Chem. Rev*, 2003, **247**, 1-19.

60 W. P. Chang, W. C. Lin, J. H. Chen, S. S. Wang and J. Y. Tung, *Dalton Trans*, 2012, **41**, 13454-13464.

61 T. Niino, M. Toganoh, B. Andrioletti and H. Furuta, *Chem. Commun*, 2006, **41**, 4335-4337.

62 M. H. Kim, T. Song, U. R. Seo, J. E. Park, K. Cho, S. M. Lee, H. J. Kim, Y.-J. Ko, Y. K. Chung and S. U. Son, *J. Mater. Chem. A*, 2017, **5**, 23612-23619.

63 A. Kempter, C. Gemel, T. Cadenbach and R. A. Fischer, *Inorg. Chem*, 2007, **46**, 9481-9487.

64 Y. Wu, Y. Zhao, R. Li, B. Yu, Y. Chen, X. Liu, C. Wu, X. Luo and Z. Liu, *ACS Catal*, 2017, **7**, 6251-6255.

65 D. J. Darensbourg, *J. Chem. Educ*, 2016, **94**, 1691-1695.

66 V. Butera, N. Russo, U. Cosentino, C. Greco, G. Moro, D. Pitea and E. Sicilia, *Chem. Cat. Chem*, 2016, **8**, 1167-1175.
67 F. Della Monica, Bholanath, T. Pehl, A. Buonerba, A. De Nisi, M. Monari, A. Grassi, B. Rieger, L. Cavallo and C. Capacchione, *ACS Catal.*, 2018, **8**, 6882-6893.
68 R. Acharya, L. Paudel, J. Joseph, C. E. McCarthy, V. R. Dudipala, J. M. Modarelli and D. A. Modarelli, *J. Org. Chem*, 2012, **77**, 6043-6050
69 O. V. Dolomanov, L. J. Bourhis, R. J. Gildea, J. A. K. Howard and H. Puschmann, *J. Appl. Cryst.*, 2009, **42**, 339-341.
70 M. C. Burla, R. Caliandro, M. Camalli, B. Carrozzini, G. L. Cascarano, L. De Caro, C. Giacovazzo, G. Polidori, D. Siliqi and R. Spagna, *J. Appl. Cryst.*, 2007, **40**, 609-613.
71 G. M. Sheldrick, *Acta Cryst*., 2015, **71**, 3-8.
72 M. J. Frisch, G. W. Trucks, H. B. Schlegel, G. E. Scuseria, M. A. Robb, J. R. Cheeseman, G. Scalmani, V. Barone, B. Mennucci, G. A. Petersson, H. Nakatsuji, M. Caricato, X. Li, H. P. Hratchian, A. F. Izmaylov, J. Bloino, G. Zheng, J. L. Sonnenberg, M. Hada, M. Ehara, K. Toyota, R. Fukuda, J. Hasegawa, M. Ishida, T. Nakajima, Y. Honda, O. Kitao, H. Nakai, T. Vreven, J. A. Montgomery, Jr., J. E. Peralta, F. Ogliaro, M. Bearpark, J. J. Heyd, E. Brothers, K. N. Kudin, V. N. Staroverov, T. Keith, R. Kobayashi, J. Normand, K. Raghavachari, A. Rendell, J. C. Burant, S. S. Iyengar, J. Tomasi, M. Cossi, N. Rega, J. M. Millam, M. Klene, J. E. Knox, J. B. Cross, V. Bakken, C. Adamo, J. Jaramillo, R. Gomperts, R. E. Stratmann, O. Yazyev, A. J. Austin, R. Cammi, C. Pomelli, J. W. Ochterski, R. L. Martin, K. Morokuma, V. G. Zakrzewski, G. A. Voth, P. Salvador, J. J. Dannenberg, S. Dapprich, A. D. Daniels, O. Farkas, J. B. Foresman, J. V. Ortiz, J. Cioslowski, and D. J. Fox, *Gaussian 09*, *Revision D.01*, Gaussian, Inc., Wallingford CT, 2013.
73 S. Grimme, J. Antony, S. Ehrlich and H. Krieg, *J. Chem. Phys.*, 2010, **132**, 154104.
74 J. Zhang, P. Yu, S.-Y. Li, H. Sun, S.-H. Xiang, J. Wang, K. N. Houk and B. Tan, *Science*, 2018, **361**, eaas8707.

View Article Online
DOI: 10.1039/C9CY00739C

Table of Contents Graphic

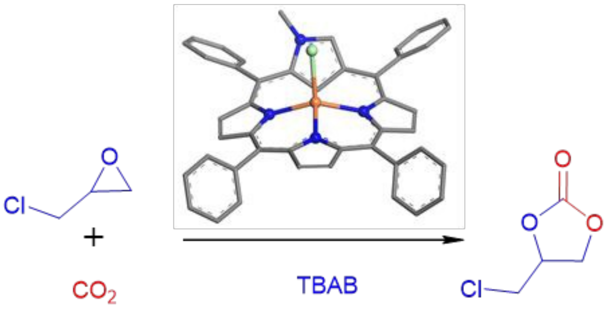

Conv.>99%, selectivity>99%, TOF=266667 h^{-1}